IOPscience iopscience.iop.org

Home Search Collections Journals About Contact us My IOPscience

Bioprinting of human pluripotent stem cells and their directed differentiation into hepatocyte-like cells for the generation of mini-livers in 3D

This content has been downloaded from IOPscience. Please scroll down to see the full text.

2015 Biofabrication 7 044102

(http://iopscience.iop.org/1758-5090/7/4/044102)

View the table of contents for this issue, or go to the journal homepage for more

Download details:

IP Address: 137.195.8.130
This content was downloaded on 23/11/2015 at 15:41

Please note that terms and conditions apply.

Biofabrication

PAPER

# Bioprinting of human pluripotent stem cells and their directed differentiation into hepatocyte-like cells for the generation of mini-livers in 3D

**Alan Faulkner-Jones**[1,2], **Catherine Fyfe**[3], **Dirk-Jan Cornelissen**[1,2], **John Gardner**[3], **Jason King**[3,4], **Aidan Courtney**[3,4] **and Wenmiao Shu**[1,2]

[1] Institute of Biological Chemistry, Biophysics and Bioengineering, School of Engineering and Physical Sciences, Heriot-Watt University, Edinburgh EH14 4AS, UK
[2] Institute of Mechanical, Process and Energy Engineering, School of Engineering and Physical Sciences, Heriot-Watt University, Edinburgh EH14 4AS, UK
[3] Roslin Cellab Ltd, Roslin BioCentre, Roslin, Midlothian EH25 9PP, UK
[4] Roslin Cells Ltd, Scottish Centre for Regenerative Medicine, Edinburgh BioQuarter, 5 Little France Drive, Edinburgh EH16 4UU, UK

**E-mail:** w.shu@hw.ac.uk

**Keywords:** 3D bioprinting, human induced pluripotent stem cells, human embryonic stem cells, stem cells, valve-based printing, hepatocyte-like cells, mini-liver

OPEN ACCESS

RECEIVED
15 April 2015

REVISED
15 June 2015

ACCEPTED FOR PUBLICATION
24 June 2015

PUBLISHED
21 October 2015

Content from this work may be used under the terms of the Creative Commons Attribution 3.0 licence.

Any further distribution of this work must maintain attribution to the author(s) and the title of the work, journal citation and DOI.

## Abstract

We report the first investigation into the bioprinting of human induced pluripotent stem cells (hiPSCs), their response to a valve-based printing process as well as their post-printing differentiation into hepatocyte-like cells (HLCs). HLCs differentiated from both hiPSCs and human embryonic stem cells (hESCs) sources were bioprinted and examined for the presence of hepatic markers to further validate the compatibility of the valve-based bioprinting process with fragile cell transfer. Examined cells were positive for nuclear factor 4 alpha and were demonstrated to secrete albumin and have morphology that was also found to be similar to that of hepatocytes. Both hESC and hiPSC lines were tested for post-printing viability and pluripotency and were found to have negligible difference in terms of viability and pluripotency between the printed and non-printed cells. hESC-derived HLCs were 3D printed using alginate hydrogel matrix and tested for viability and albumin secretion during the remaining differentiation and were found to be hepatic in nature. 3D printed with 40-layer of HLC-containing alginate structures reached peak albumin secretion at day 21 of the differentiation protocol. This work demonstrates that the valve-based printing process is gentle enough to print human pluripotent stem cells (hPSCs) (both hESCs and hiPSCs) while either maintaining their pluripotency or directing their differentiation into specific lineages. The ability to bioprint hPSCs will pave the way for producing organs or tissues on demand from patient specific cells which could be used for animal-free drug development and personalized medicine.

## 1. Introduction

New drug development can take 10 to 20 years with an estimated average of about 9 to 12 years [1, 2]. In addition, only around 16% of the drugs that begin preclinical testing are approved for human use [3]. Some of this low success rate can be attributed to the different responses that animals and humans have to the drugs being tested; some drugs have to be withdrawn from market due to toxic effects on human organs such as liver and heart, despite being tested safely on animals. A possible solution to this might be the creation of human pluripotent stem cell (hPSC) -derived micro-tissues which could be used with organ-on-a-chip devices [4–7]. These micro-tissues are expected to produce the same or similar physiological reaction that the entire organ would but on a much smaller scale. This would result in scalable, faster and potentially more reliable drug testing platform, and hopefully an end to animal testing.

hPSCs are the ideal cells to use for this application due to their ability to self-renew indefinitely, which enables large populations of cells to be created easily *in vitro*, and their pluripotency which means that they

© 2015 IOP Publishing Ltd

can be differentiated into any required adult cell type [8–13]. Pluripotent stem cells can be divided into embryonic stem cells (ESCs) and induced pluripotent stem cells (iPSCs). Human ESCs (hESCs) were first isolated from early human blastocysts in 1998 [14]. Any tissue construct created from hESCs for implantation in vivo would require the patient to receive immunosuppressive drugs and ethical issues still restrict some applications due to their source. iPSCs have neither of these drawbacks as they can be created from harvested adult cells from the patient requiring treatment and as such any implanted cells derived from these iPSCs should not be rejected by the patient's immune system but may require immunosuppressive drugs at a greatly reduced dosage. In 2006 Shinya Yamanaka discovered that iPSCs can be derived from somatic cells by retrovirally transducing them with four transcription factors—Oct3/4, Sox2, Klf4 and C-myc [15, 16]. These cells have the same self-renewal and differentiation capabilities as ESCs but with the added advantage that iPSCs can be used for autologous therapies. These unique characteristics make pluripotent stem cells ideal for use in a number of applications such as clinical tissue engineering, novel drug discovery and testing for the pharmaceutical industry [8, 9, 17, 18].

In the field of biofabrication, great advances are being made towards fabricating 3D tissue and organs with very fine spatial control of cell deposition. From the very first paper that was published investigating printing of biological cells (or bioprinting), tissue engineering was identified as a major application for this new technology [19]. If more complex structures such as organs and tissues were to be printed, the bioprinter would need the ability to transfer microscopic patterns of viable cells of multiple cell types into well-defined three-dimensional arrays that closely mimic the tissue structure. There has been much progress in the development and establishment of several different bioprinting techniques for 3D live constructs [20–22] including those based on laser pulses, inkjets and other more novel approaches. It is an inescapable fact that cells will be subjected to some level of stress during deposition, regardless of the printing technique being used. For example, cells printed by non-contact methods will be affected when they impact on the substrate at some incident velocity, which would result in extreme deceleration and shear stress [23–26]. Shear stress is applied to cells pushed through nozzle orifices and capillary tubes [24, 27–42] and the actuation is provided via pressure, heat, or high frequency vibration which can also be damaging to the cells [30, 31, 43–46]. If cells are exposed to laser energy the radiation can cause genetic damage [29, 47–54] and shear forces are applied during cavitation and jet formation [23, 55]. Ultrasonic actuation for cell transfer would subject the cells to stress in the form of heat and vibration [56, 57]. Therefore, it is important to validate the response of printed cells to any particular bioprinting process in terms of their viability and more importantly their biological functions.

We previously reported the results of the first experiments printing hESCs using a valve-based printing approach including their response to the printing process in the form of post-printed viability and pluripotency validation [37]. However, if hPSCs are to be used for producing human tissues on demand for drug testing, their post-printing differentiation must be reproducibly directed to the required lineages for each tissue. Unfortunately homogenous cellular differentiation of hPSCs into some germ layers has proved difficult [12, 13]. Here, we report the first investigation into the bioprinting of human iPSCs, their response to the valve-based printing process as well as their post-printing differentiation into hepatocyte-like cells (HLCs). HLCs that are in the process of differentiating are bioprinted and examined to further validate the compatibility of the valve-based bioprinting process with fragile cell transfer. Finally, 3D hydrogel structures were designed and printed out with encapsulated hESC-derived HLCs and the viability and hepatic characteristics of the cells were investigated.

## 2. Materials and methods

### 2.1. Cell culture

Human induced pluripotent stem (hiPS) cell lines RCi-22 and RCi-50 and hESC lines RC-6 and RC-10 were supplied by Roslin Cells Ltd for this research. The hiPS cells were cultured on Geltrex matrix with Essential 8 medium (Life Technologies) and the hES cells were cultured in complete StemPro® hESC serum-and feeder-free medium (SFM) (supplement, DMEM/F-12, BSA, FGF basic, and 2-mercaptoethanol) (Life Technologies) supplemented with 8 ng $mL^{-1}$ of human basic fibroblast growth factor. Cells were cultured in a laboratory incubator set at 36.0 °C–37.5 °C, 5.0% $\pm$ 0.5% $CO_2$.

### 2.2. Cell printing platform

A newer version of our previously reported cell printing platform [37] has been developed. Four nanolitre dispensing systems, each comprising a solenoid valve (VHS Nanolitre Dispense Valve, Lee Products Ltd) with 101.6 $\mu$m internal diameter nozzles (Minstac Nozzle, Lee Products Ltd), were attached to static pressure reservoirs for the bio-ink solution to be dispensed from via flexible tubing. The nanolitre dispensing system and bio-ink reservoirs were mounted onto the tool head of an enclosed custom built micrometer-resolution 3-axis *XY–Z* stage (figure 1). This newer cell printing platform improved on the previous version by reducing the overall size and weight of the machine, allowing it to be mounted inside a standard tissue culture hood during experiments requiring a sterile environment. Other enhancements included the two extra nanolitre

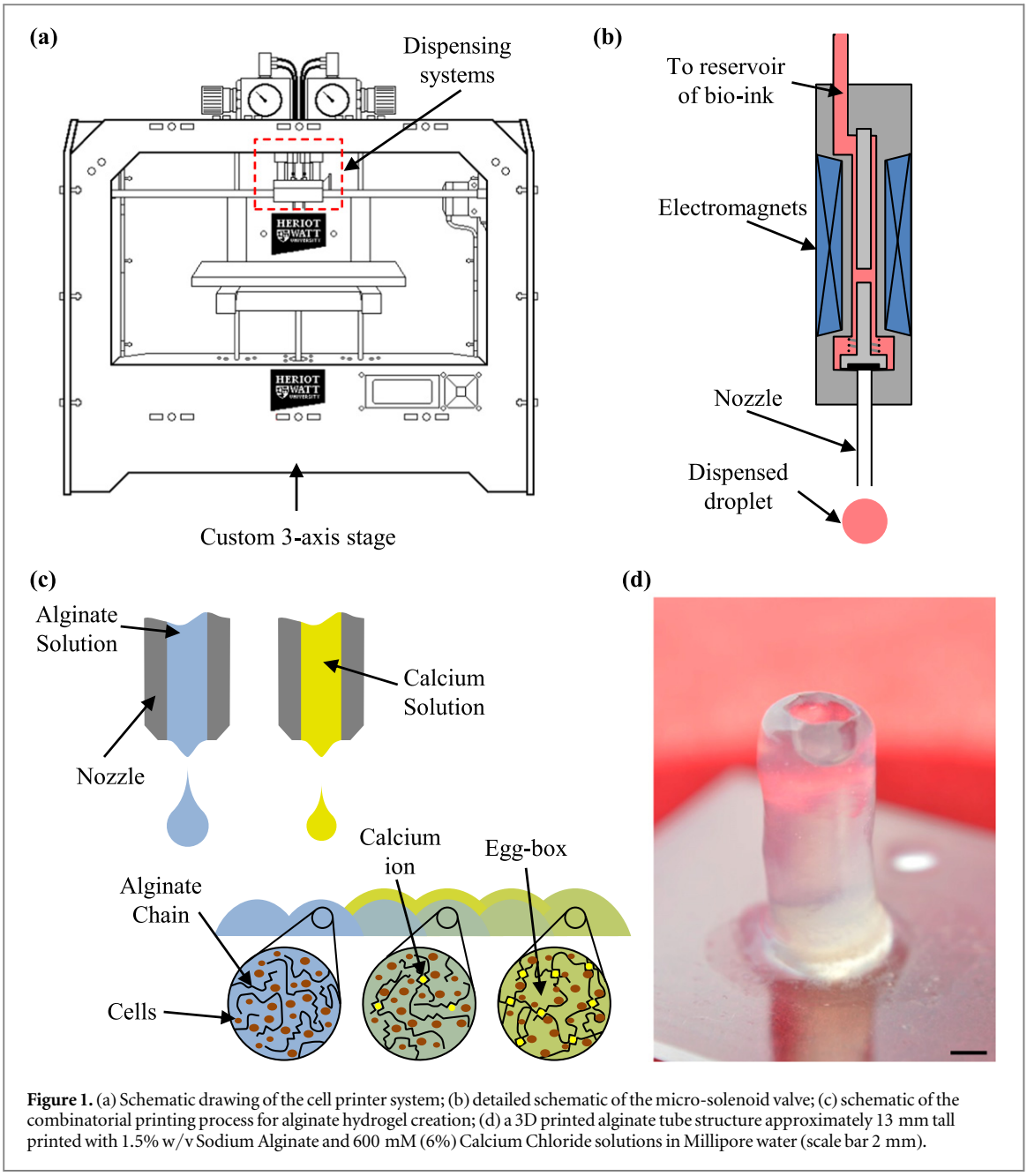


**Figure 1.** (a) Schematic drawing of the cell printer system; (b) detailed schematic of the micro-solenoid valve; (c) schematic of the combinatorial printing process for alginate hydrogel creation; (d) a 3D printed alginate tube structure approximately 13 mm tall printed with 1.5% w/v Sodium Alginate and 600 mM (6%) Calcium Chloride solutions in Millipore water (scale bar 2 mm).

dispensing systems, taking the total up to four, a more robust electronics and custom firmware was developed which improved the reliability and speed of the machine and two separate pressure channels were included, allowing for differential bio-ink dispensing conditions. Unless otherwise stated standard printing conditions were used: for 2D, printing was carried out using a pulse time of 8 ms at an inlet pressure of 0.6 bar using a nozzle with an internal diameter of 101.6 $\mu$m; for 3D, printing was carried out using a pulse time of 400 $\mu$s at an inlet pressure of 1.0 bar for sodium alginate solution and a pulse time of 400 $\mu$s at an inlet pressure of 0.5 bar for calcium chloride solution both using nozzles with an internal diameter of 101.6 $\mu$m.

### 2.3. Bioprinter sterilization and validation

The bioprinting system was sterilized and rinsed with a 2% solution of Presept (Johnson and Johnson Medical) (left to stand for 30 min), a 70% solution of Ethanol and water (all micro-filtered), then Tryptose Phosphate broth (Sigma-Aldrich Co. LLC) was printed into the wells of a 96-well plate for testing. The plate was incubated in a $CO_2$ incubator (Galaxy S+, RS Biotech) at 36.0 °C–37.5 °C, 5.0% ± 0.5% $CO_2$ and checked for microbial growth every 72 h for 21 d.

### 2.4. Cell viability

Human ES cells (line RC-10) were suspended in StemPro® hESC SFM to a concentration of approximately $1 \times 10^6$ cells/mL, loaded into the reservoir of one of the cell deposition systems and dispensed in approximately 1 mL increments of bio-ink (the volume varied with pressure) using a previously written program; this large volume was required to allow for analysis to be carried out on a fluorescence-activated cell sorting (FACS) flow cytometer.

Different experiments sometimes require different experimental variables such as applied pressure and nozzle geometry. Two main types of nozzle have been used for the experiments: a shorter, thick-walled nozzle; and a longer, thin-walled nozzle. The shorter nozzle measured 8.9 mm in length while the longer nozzle measured 24.4 mm. Since such a large volume was required for each pressure/nozzle combination, only four different pressures were used to limit the number of cells required for this experiment. Cells were printed into micro-centrifuge tubes and the unprinted cells were used as a control.

The printed samples were examined using a BD FACS Calibur flow cytometer (BD Cell Viability Kit) at approximately 30 min post printing. The control sample was split in two; half was used to calibrate the data thresholds.

Human iPS cells (line RCi-22) viability was measured in much the same way as the hESC viability but without a variation in nozzle geometry or pressures. The printed samples were examined using the flow cytometer.

### 2.5. Multi-marker pluripotency validation hESC (RC-10) and human induced pluripotent stem cells (hiPSC) (RCi-22)

Cells were printed directly into the wells of 12-well plates and cultured in a $CO_2$ incubator (Galaxy S+, RS Biotech) at 36.0 °C–37.5 °C, 5.0% ± 0.5% $CO_2$ for one week. The now adherent hPSCs were washed once with PBS and Tryple select (Invitrogen) was added to detach the cells from the surface and return them to a single cell suspension. A sample was viewed under the microscope to confirm the presence of single cells. Cells were then washed three times with PBS and centrifuged at 300 g for 5 min before being re-suspended in an appropriate volume of PBS for the required cell concentration.

Cells were fixed using BD Cytofix™ for 20 min at room temperature (RT). Cells were permeabilised by washing twice with 1X BD Perm/Wash buffer (centrifuging at 500 g for 5 min), re-suspended in 1X BD Perm/Wash buffer at $1 \times 10^7$ cells/mL and then incubated for 10 min at RT.

Printed and control samples were analyzed using a FACS machine (FACSCalibur, BD) according to the BD human and mouse pluripotent stem cell analysis protocol.

### 2.6. Directed differentiation of hPSCs into HLCs

We used a modified version of the three-step protocol devised by Hay *et al* [13] to direct the differentiation of hPSCs into HLCs; this protocol is shown in figure 2. In brief, cells are seeded at a specific initial concentration in StemPro® hESC SFM, after 24 h this medium was replaced with RPMI-B27 medium (Invitrogen) and the hESCs were treated with Activin A and Wnt 3a for 3 d. Following this, the cells were cultured in serum replacement medium (SR/DMSO: knockout-Dulbecco's modified Eagle's medium containing 20% SR, 1 mm Glutamine, 1% non essential Amino Acids, 0.1 mM $\beta$-Mercaptorthanol, and 1% DiMethyl Sulfoxide [DMSO]) for 5 d. For the final maturation step cells were cultured in L15 medium supplemented with 8.3% Fetal Bovine Serum, 8.3% Tryptose Phosphate broth, 10 $\mu$M Hydocortisone 21-hemisuccinate, 1 $\mu$M Insulin, and treated with 10 ng mL$^{-1}$ Hepatocyte Growth Factor and 20 ng mL$^{-1}$ Oncostatin M for 9 d.

### 2.7. HNF4$\alpha$ and albumin Immunofluorescence

The cells should be positive for hepatocyte nuclear factor 4 alpha (HNF4$\alpha$) if they have started differentiating into hepatocytes. As the cells mature they should begin to express albumin, which can only be synthesized in large quantities by mature hepatocytes (immature hepatocytes also express albumin but at much lower levels) [13, 58]. On completion of the differentiation process, cells were washed in PBS and fixed using 4% Paraformaldehyde for 20 min at RT. Cells were permeabilised by washing in PBST (PBS plus 0.1% Tween20) and blocked using 10% normal goat serum (NGS) (G9023, Sigma-Aldrich Co. LLC) in PBST for 1 h at RT. Blocking buffer was then replaced using antibody diluent buffer (1% NGS) and the appropriate primary antibody. HNF4$\alpha$ rabbit polyclonal IgG (SC8987, Santa Cruz Biotechnology Inc.) at a dilution of 1:100 or human serum albumin IgG2a mouse monoclonal (A6684, Sigma-Aldrich Co. LLC) at a dilution of 1:500 or ZO-1 IgG rabbit polyclonal (SC10804, Santa Cruz Biotechnology Inc.) at a dilution of 1:50. This was incubated overnight at 2 °C–8 °C. Primary antibody was removed by washing three times with PBST for 5 min each at RT. Secondary antibodies for HNF4$\alpha$ and ZO-1- goat anti rabbit IgG (ab96884, Abcam plc.) and human serum albumin-goat anti mouse IgG (A11029, Life Technologies) were diluted 1:200 in PBST and were used for 1 h at RT in the dark on a rocker table. Unbound antibody was removed during three 5 min PBS washes on a rocker table at RT in the dark. Samples were then counterstained using DAPI before being analyzed on a fluorescence microscope.

### 2.8. Albumin ELISA

Cell culture supernatants were collected from non-printed control and 3D bioprinted structures on day 12,16,19,21 and 23 of the differentiation process. Albumin secretion was detected and quantified using a human albumin ELISA (ab108788, Abcam plc.) used according to manufacturer's instructions.

### 2.9. 3D bioprinting using alginate hydrogel

Alginate is a natural linear polysaccharide copolymer which is extracted from brown seaweed algae. Due to their biocompatibility, non-immunogenicity, low toxicity and hydrophilic nature, alginate hydrogels

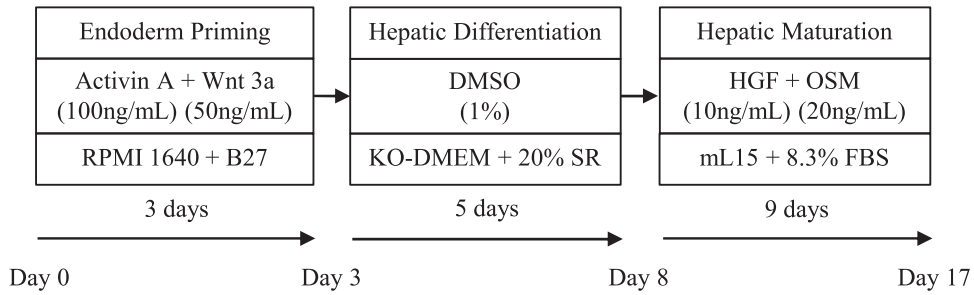


**Figure 2.** A schematic representation of the three-step protocol used to differentiate hPSCs into HLCs detailing the media changes and treatments required for each stage.

have many attractive features for biomedical applications [59]. The mechanical properties of a gelled alginate solution, including viscosity and overall stiffness, depend on the concentration of the polymer and its molecular weight distribution [60, 61]. Crosslinking between the polymer chains depends on the amount of polymer chains and multivalent cations (e.g. $Ca^{2+}$, $Ba^{2+}$) present in the solution and the temperature [59–62]. *In vitro*, alginates typically degrade by approximately 40% within 9 d; this is most likely due to the diffusion of ions into the surrounding medium [63].

RGD-coupled sodium alginate (NOVATACH GRGDSP, Novamatrix), Calcium chloride dihydrate (223506, Sigma-Aldrich Co. LLC), and Barium chloride (B0750, Sigma-Aldrich Co. LLC) were used to form alginate hydrogels. RGD-coupled alginate was used for its known bio-compatibility with stem cells [64]. Alginate hydrogel structures are bioprinted by dispensing an array of droplets of alginate solution from the left nozzle and then overprinting droplets of calcium solution from the right. After a few seconds the alginate chains bond with the calcium ions to form a hydrogel matrix. If adjacent droplets overlap they gel together and form a single continuous layer. Additionally, by exposing the printed hydrogel structures to barium chloride the structural integrity will increase.

$5 \times 10^6$ hESC-HLCs at day 6 of the differentiation protocol were suspended in 0.5 mL 1.5% w/v sodium alginate resulting in a concentration of $1 \times 10^7$ cells/$mL^{-1}$. 60 mM calcium chloride was used as the cross-linker. Programs describing 3D ring structures with a range of layer heights and diameters were created for the bioprinter. These ring structures were then printed out using the HLC-laden alginate into the wells of 12-well plate. After printing, the cell laden hydrogel structures were exposed to barium chloride (55 mM) for 2 min Differentiation media was then added to the printed structures and the cells were allowed to continue their differentiation to day 17 suspended in the alginate. The plates were incubated in a $CO_2$ incubator (Galaxy S+, RS Biotech) at 36.0 °C–37.5 °C, 5.0% ± 0.5% $CO_2$. At day 17 a number of structures were dissociated using 55 mM EDTA to allow for examination of hepatic markers.

### 2.10. 3D imaging and viability measurement

Confocal laser scanning microscopy (CLSM) (Leica SP5 SMD; Leica microsystems) was used for 3D image acquisition. Images were taken using a dry 20X objective. CLSM images were analyzed using Imaris (Bitplane, AG) software to investigate the viability of the bioprinted cells post-printing and end of the differentiation process.

## 3. Results and discussion

### 3.1. Bioprinter sterilization and validation

Producing human tissue from pluripotent stem cells requires the printed samples to be cultured post-printing for several weeks to allow the cells to differentiate into the required lineages. Creation of tissue from stem cells using bioprinting techniques usually involve a lengthy culture periods which can last from several weeks up to months in some cases [65–67], so it was important to ensure that not only would these cells be unaffected by the printing process but that no microbial contamination entered the system and affected the results. Therefore the bioprinter was thoroughly cleaned, placed in a Class II microbiological safety cabinet and tested for sterility using Tryptose Phosphate broth. The broth-populated plate was removed from the incubator and examined at three day intervals up to 21 d post-printing and there was no evidence of microbial contamination present therefore the system was deemed to be sterile. Sterilization is essential for long term culture and as the differentiation protocol for HLCs lasts for 17 d, it is crucial that the printer does not introduce foreign contaminants into the culture environment which might influence the differentiation of the stem cells. Even without the use of antibiotics, samples printed using our bioprinting system remained sterile for at least three weeks.

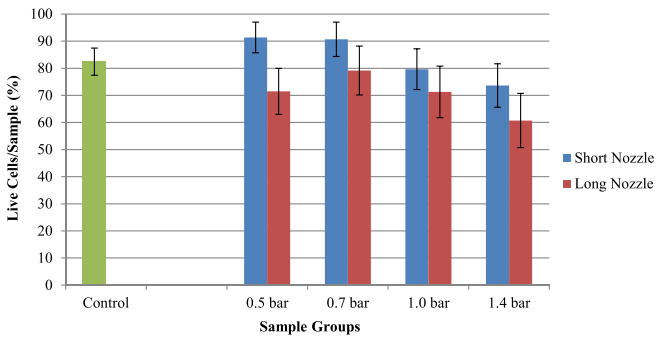


**Figure 3.** A graph to show the post printing viability of hESCs per sample as a function of pressure and nozzle length.

### 3.2. The effect of pressure and nozzle length on hESC viability

We previously demonstrated that hESCs bioprinted using valve-based techniques retain high viability post-printing using trypan blue exclusion [37]. Here, we further confirm this result by carrying out a more systematic study using FACS, which yields more statistically significant results to the previous study, and expand the study by examining the effect of different nozzle lengths on post-printed viability of hESCs. Other groups have previously examined the effects of nozzle diameter on cell viability [68–71], but the effect of nozzle length on cell viability has not been investigated. The two nozzles used in this study measured 8.9 and 24.4 mm in length. The graph of the results is shown in figure 3. These results clearly show that increased pressure results in lower cellular viability; this can be attributed to the higher shear forces applied to the cells as they are printed. However cell viability remains high at pressures below 1 bar even for sensitive cells such as hESCs, which is consistent with the observations of other groups with stem cells [72] and other cell types using similar bioprinting approaches [68, 69].

Cell viability was calculated to be >84% for the short nozzle and >71% for the long nozzle over all pressures. This clearly shows that the viability of the cells is affected by the length of the nozzle used; this is most likely due to the increased time the cells are subject to shear forces through the nozzle. We speculate that the higher viability of hESCs (RC-10 in this case) post-printing as compared to the non-printed control might be due to printing induced homogenizing of the cell suspensions; live hESCs tend to aggregate into small clumps which could be falsely identified as single cells in control solutions but be broken up during printing and counted separately.

### 3.3. hPSC viability post printing

Using the results shown in figure 3, the optimal printing conditions were set at 0.6 bar and the shorter nozzle was used. Using these parameters, we compared the viability of hESC and hiPSC post printing. The data plots and a graph of the results are shown in figure 4. There is negligible difference in terms of viability between the printed and non-printed hiPSCs and there is actually an increase in viability between the printed and non-printed hESCs which shows that our valve-based printing technology is compatible with hPSC transfer without affecting the viability of these fragile cells.

### 3.4. Multi-marker pluripotency validation

Viability alone is insufficient when printing pluripotent stem cells; printed cells must not only be viable but also morphologically unchanged by the printing process. In other words, they need to still be pluripotent stem cells post-printing; the bioprinting process must not trigger the cells to differentiate. Pluripotency can be validated by testing cells for the presence of certain biomarkers including SSEA-3, SSEA-4, OCT3/4, SOX2, NANOG and many others [15, 73]. The printed cells were examined to verify that they still possessed two of the most common pluripotency markers: Oct3/4 and SSEA-4. SSEA-1 (stage-specific embryonic antigen 1) was used as a negative test as it should only be expressed in differentiated cells.

The results are shown in figure 5. At one week post-printing there is little observable difference between the printed cells and the non-printed control which confirms that all the tested hPSCs remain pluripotent. The Oct3/4 marker levels are lower than the normal range for pluripotency in the printed RC-10 and RCi-22 while still being acceptable. The RC-6 SSEA-4 printed result is lower than the control but the results are still positive and they are within an acceptable range.

### 3.5. Printed hPSC-derived hepatocytes

HLC's progressed to day 6 of the differentiation protocol were used to determine the effect of bioprinting on cell differentiation in terms of hepatic parkers. Day 6 HLCs were harvested, dissociated into single cells and printed into the wells of a 12-well plate. After printing the differentiation protocol was resumed

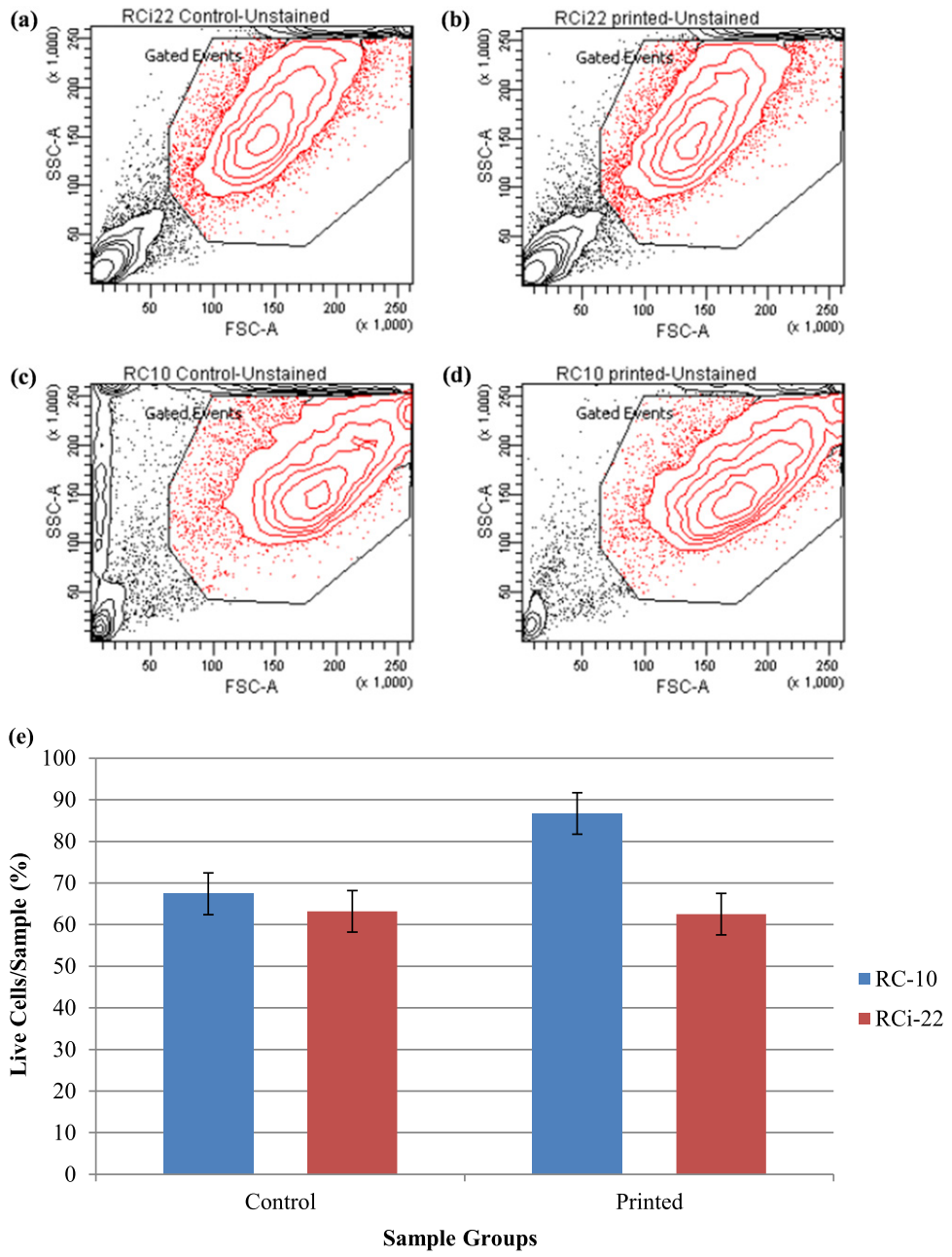


**Figure 4.** Flow cytometry data plots showing the numbers of live hiPSCs per sample with numbers of hESCs per sample for comparison: ((a) and (b)) hiPSC line RCi-22: (a) control; (b) printed cells; ((c) and (d)) hESC line RC-10: (c) control; (d) printed cells; (e) aa graph to show the percentages of live hiPSCs per sample with hESC results for comparison.

until day 17 after which the cells were tested for the presence of albumin and HNF4$\alpha$, ZO-1 was used to check the morphology of the cells.

Both hESC- and hiPSC-derived HLCs were bioprinted and the results are shown in figure 6. When the cells were compared to an unprinted control all hepatic markers were expressed indicating that cells can be printed during the directed differentiation process without interrupting the differentiation or changing the lineage of the cells. This is an important result as it means that these cells can be patterned in three-dimensions using our bioprinter while differentiating which will greatly speed up the creation of mini-liver tissue structures.

### 3.6. 3D Bioprinting with hydrogel

Sodium alginate solutions with concentrations from 0.1% to 5% were successfully dispensed using the bioprinter at inlet pressures of 0.1–1 bar. The calcium solution has a much lower viscosity and should therefore be dispensed at much lower pressures in order to avoid flooding the printed hydrogel structure with excess calcium solution.

The process of *in vivo* liver organogenesis occurs in the developing foregut, when newly specified hepatic cells separate from the endodermal sheet and form a dense 3D structure known as a hepatoblast (liver bud) [74, 75]. It is hypothesized that arranging the hESC–HLCs in 3D during the differentiation process may

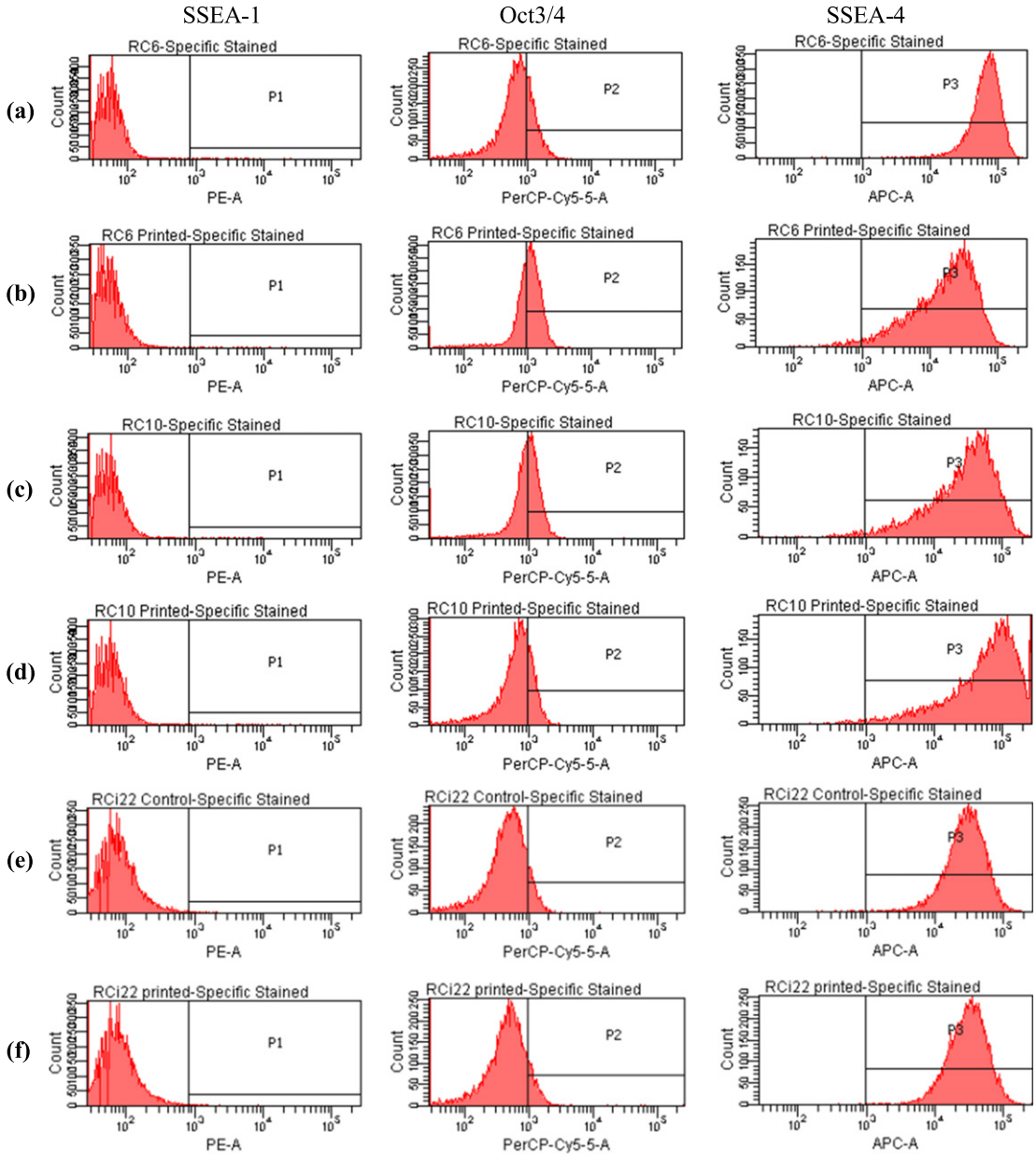


**Figure 5.** FACS results of multi-marker pluripotency validation: (a) and (b) hESC line RC-6: (a) non-printed control; (b) printed results; ((c) and (d)) hESC line RC-10: (c) non-printed control; (d) printed results; ((e) and (f)) hiPSC line RCi-22: (e) non-printed control; (f) printed results.

yield more mature hepatocytes than conventional 2D differentiation. The hESC differentiation protocols are more efficient and robust than hiPSC protocols therefore only hESC-derived HLCs were printed in 3D.

In order for this technique to be useful for tissue engineering applications, structures need to be tall enough to allow cells to interact in a three-dimensional environment. The concentration of alginate solution was set to 1.5% w/v to improve the mechanical strength of the hydrogel and allow it to support further layers. Circular structures with a large number of layers were designed and printed out in the wells of a multi-well plate to allow the structures to be cultured post-printing. These resulting structures were photographed for analysis and are shown in figure 7 below.

These structures were printed out in a matter of minutes and are strong enough to support their own weight and the weight of further layers (as seen in figure 1(d)). The structures spread slightly, but by slightly altering the volume ratio, concentrations and surface properties this spreading can be reduced.

Approximately one hour post-printing one of the HLC-laden alginate ring structures was examined using a confocal microscope; the 3D image is shown in figure 8(a). Cell viability was calculated to be 55.5% using the Imaris confocal microscope software. Cell viability declined over the first 24 h which resulted in low cell numbers for hepatic marker testing following the 3D differentiation process, but the viability remained stable for the remainder

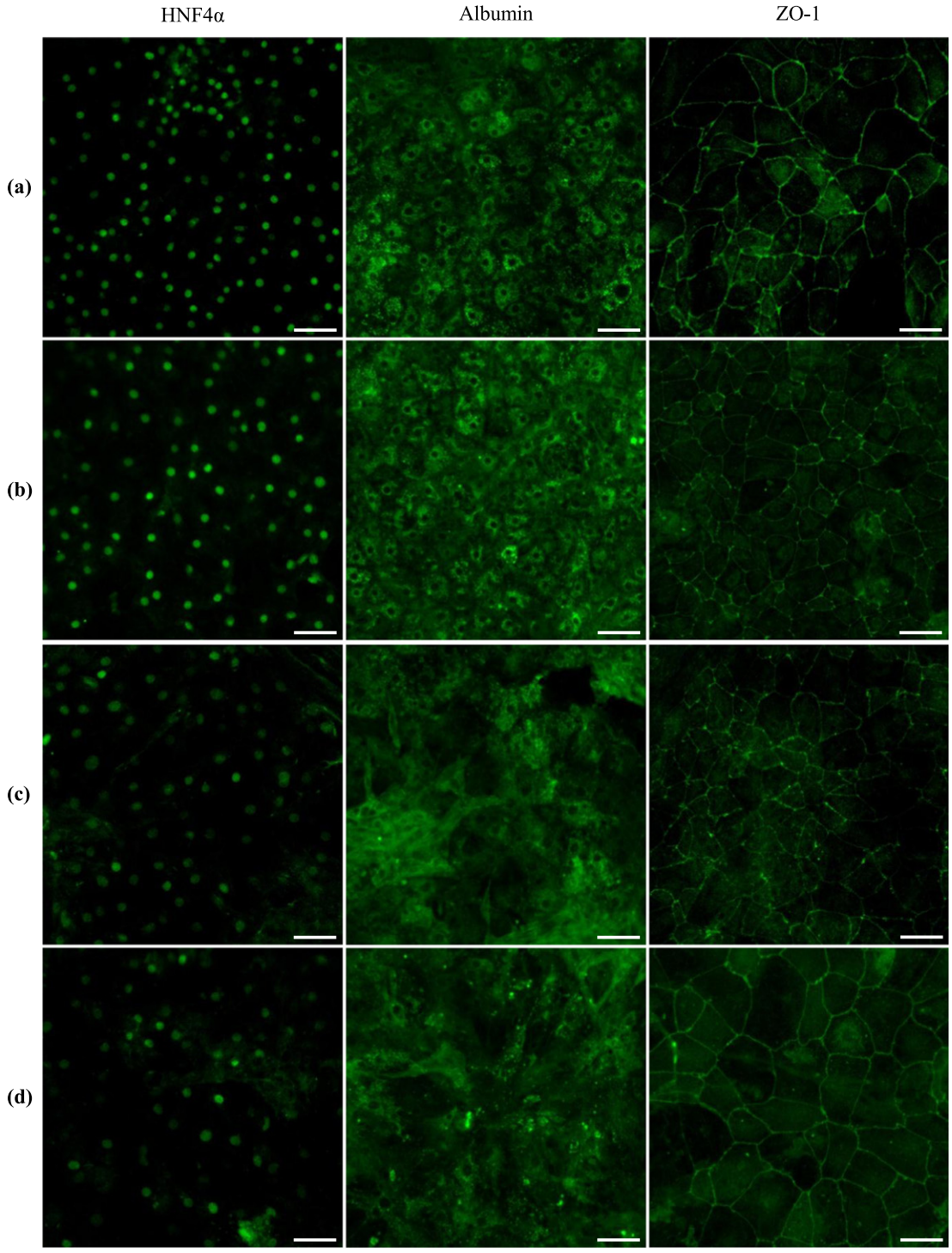


**Figure 6.** Fluorescence images of printed hPSC-derived hepatocytes showing hepatocyte marker expression in green: ((a) and (b)) hESC-derived HLCs (RC-10): (a) non-printed control; (b) printed results; ((c) and (d)) hiPSC-derived HLCs (RCi-22): (c) non-printed control; (d) printed results (scale bars 50 $\mu$m).

of the differentiation process. At day 23 of the differentiation process, the cells in the remaining structures were harvested and stained for the presence of hepatic markers. As shown in figure 8(b), cells are positive for albumin which demonstrates their hepatic lineage. The normal time required for 2D differentiation of hPSC-HLCs is 17–24 d. However, based on the results of albumin secretion in the medium, we observed the 3D printed cells have taken longer to reach the maximum albumin secretion than the 2D control as shown in figure 8(c). Interestingly, when analyzing the difference between 20 and 40 layer printed tube structures, we noticed close-to proportional increase in albumin secretion to the number of layers as shown in figure 8(d). This indicates that the permeability of the alginate hydrogel allows nutrition and differentiation reagents to enter the structure and

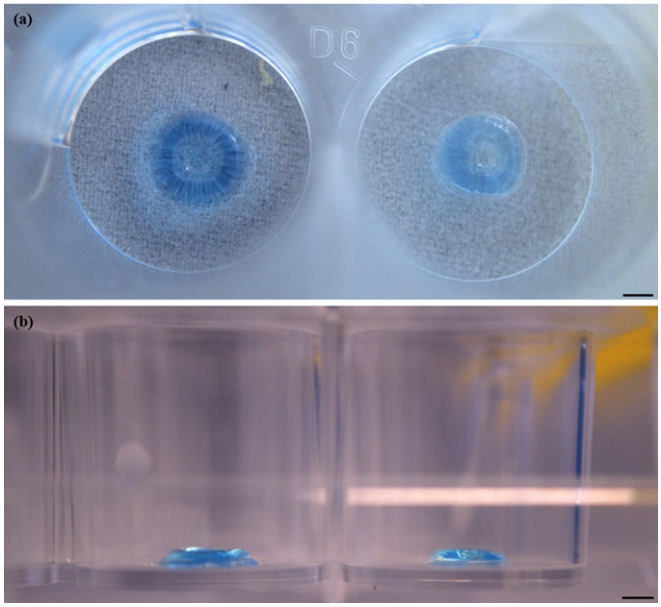


**Figure 7.** 3D printed alginate ring structures with 40 layers printed into the wells of a 24-well plate with blue dye added for visual clarity: (a) top view; and (b) side view (scale bar 2 mm).

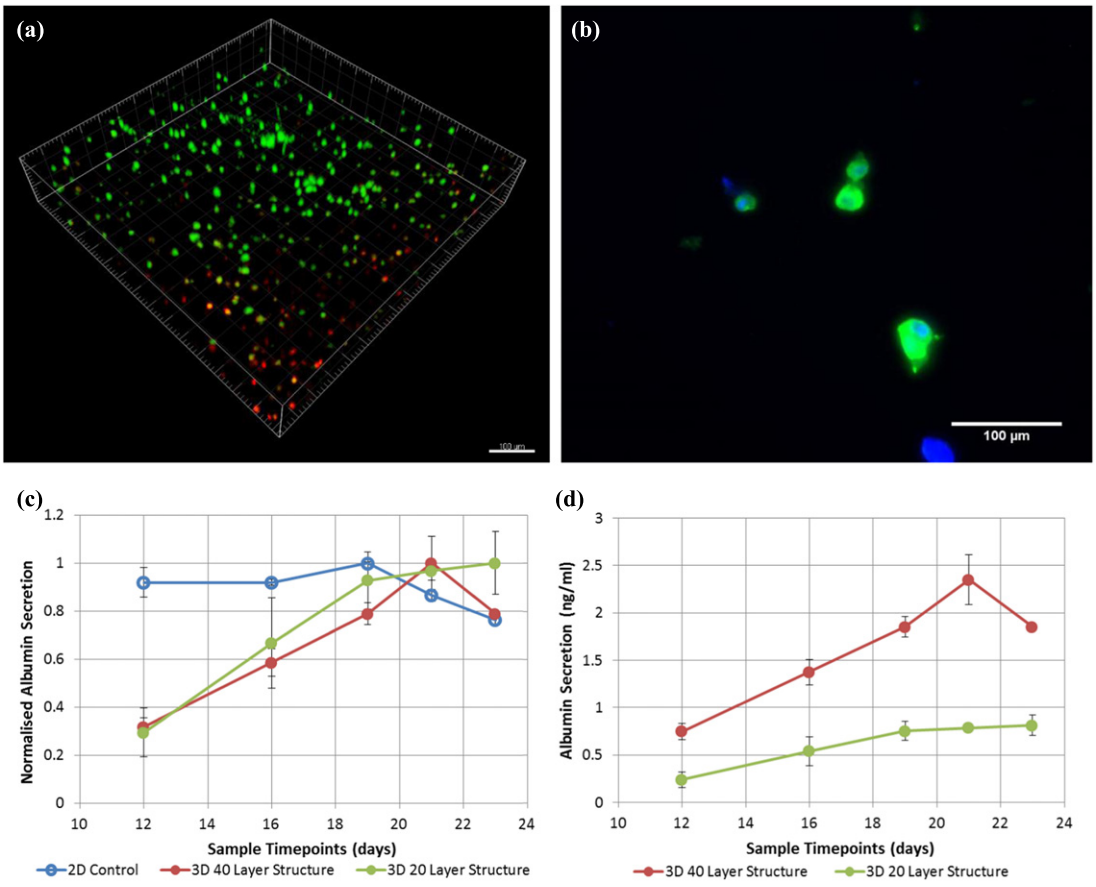


**Figure 8.** ((a) and (b)) Fluorescence images of printed hESC-derived hepatocytes: (a) a 3D stack of HLCs printed in hydrogel, recorded one hour post-printing showing live cells in green and dead cells in red; (b) 2D cells harvested from the alginate at day 23 showing albumin expression in green and DAPI in blue (scale bars 100 $\mu$m); ((c) and (d)) graphs of albumin secretion at set points during the directed differentiation process for two 3D printed structures with 40 and 20 layers as well as a 2D control: (c) normalized albumin secretion which shows the 40 layer 3D printed structure reaches peak albumin secretion after the 2D control (shown here at day 21 and day 19 respectively); (d) a comparison between the absolute albumin secretion of the two 3D printed structures which shows that greater number of printed cells printed leads to higher albumin secretion.

support 3D differentiation and maturation processes of the cells, regardless of the height of the printed structure.

Research is currently underway including investigations to improve the 3D viability and adjusting the differentiation protocol that may facilitate higher albumin secretion. For example, the optimization of hydrogel formation as well as enhanced cell density may improve the differentiation process for hPSCs in 3D [21, 76, 77].

## 4. Conclusions

To the best of our knowledge, this study is the first to demonstrate that hiPS cells can be bioprinted without adversely affecting their biological functions including viability and pluripotency. Importantly, we verified that our valve-based printing process is gentle enough to not affect the pluripotency of both hESCs and hiPSCs. A number of different hPSC lines were directed to differentiate into HLCs. Cells were printed during the differentiation process and showed no differences in hepatocyte marker expression and similar morphology when compared to a non-printed control. We previously reported the results of an investigation into the response of hESCs to the valve-based printing process. Here we build on that study, performing a deeper investigation to compare the response of hiPSCs and hESCs to the printing process using flow cytometry. The effect of nozzle geometry was investigated and the effects of nozzle length on the post-printing viability of cells were recorded; longer nozzles lower the post-printing viability of the cells. We printed hESC-derived HLCs in a 3D alginate matrix and tested for viability and hepatic markers during the remaining differentiation and they were found to be hepatic in nature. The ability to bioprint hPSCs while either maintaining their pluripotency or directing their differentiation into specific cell types will pave the way for producing organs or tissues on demand from patient specific cells which could be used for animal-free drug development and personalized medicine.

## Acknowledgments

The authors acknowledge the funding support from the EPSRC (Grant No. EP/M506837/1), Innovate UK and NC3Rs (Advancing the development and application of non-animal technologies program) as well as the Scottish Universities Physics Alliance (SUPA)'s INSPIRE scholarship sponsored by the Scottish Funding Council. The authors would also like to thank William Ramsay, Yijie Wang and the Edinburgh Super-resolution Imaging Consortium (ESRIC) for their assistance in some of the experimental work.

## References

[1] Dickson M and Gagnon J P 2009 The cost of new drug discovery and development *Discov. Med.* **4**(**22**) 172–9
[2] Kaitin K 2010 Deconstructing the drug development process: the new face of innovation *Clin. Pharmacol. Ther.* **87** 356–61
[3] Paul S M, Mytelka D S, Dunwiddie C T, Persinger C C, Munos B H, Lindborg S R and Schacht A L 2010 How to improve R&D productivity: the pharmaceutical industry's grand challenge *Nat. Rev. Drug Discov.* **9** 203–14
[4] Kolaja K 2014 Stem cells and stem cell-derived tissues and their use in safety assessment *J. Biol. Chem.* **289** 4555–61
[5] Huh D, Matthews B D, Mammoto A, Montoya-Zavala M, Hsin H Y and Ingber D E 2010 Reconstituting organ-level lung functions on a chip *Science* **328** 1662–8
[6] Jensen J, Hyllner J and Björquist P 2009 Human embryonic stem cell technologies and drug discovery *J. Cell. Physiol.* **219** 513–9
[7] Chang R, Emami K, Wu H and Sun W 2010 Biofabrication of a three-dimensional liver micro-organ as an *in vitro* drug metabolism model *Biofabrication* **2** 045004
[8] Murry C E and Keller G 2008 Differentiation of embryonic stem cells to clinically relevant populations: lessons from embryonic development *Cell* **132** 661–80
[9] Fenno L E, Ptaszek L M and Cowan C A 2008 Human embryonic stem cells: emerging technologies and practical applications *Curr. Opin. Genet. Dev.* **18** 324–9
[10] Itskovitz-Eldor J, Schuldiner M, Karsenti D, Eden A, Yanuka O, Amit M, Soreq H and Benvenisty N 2000 Differentiation of human embryonic stem cells into embryoid bodies compromising the three embryonic germ layers *Mol. Med.* **6** 88–95
[11] Gage F H 2000 Mammalian neural stem cells *Science* **287** 1433–8
[12] Hay D C *et al* 2008 Highly efficient differentiation of hESCs to functional hepatic endoderm requires ActivinA and Wnt3a signaling *Proc. Natl Acad. Sci.* **105** 12301–6
[13] Hay D C *et al* 2008 Efficient differentiation of hepatocytes from human embryonic stem cells exhibiting markers recapitulating liver development *in vivo Stem Cells* **26** 894–902
[14] Thomson J A, Itskovitz-Eldor J, Shapiro S S, Waknitz M A, Swiergiel J J, Marshall V S and Jones J M 1998 Embryonic stem cell lines derived from human blastocysts *Science* **282** 1145–7
[15] Takahashi K, Tanabe K, Ohnuki M, Narita M, Ichisaka T, Tomoda K and Yamanaka S 2007 Induction of pluripotent stem cells from adult human fibroblasts by defined factors *Cell* **131** 861–72
[16] Takahashi K and Yamanaka S 2006 Induction of pluripotent stem cells from mouse embryonic and adult fibroblast cultures by defined factors *Cell* **126** 663–76
[17] McNeish J 2004 Embryonic stem cells in drug discovery *Nat. Rev. Drug Discov.* **3** 70–80
[18] Wu D C, Boyd A S and Wood K J 2007 Embryonic stem cell transplantation: potential applicability in cell replacement therapy and regenerative medicine *Front. Biosci.* **12** 4525–35
[19] Klebe R J 1988 Cytoscribing: a method for micropositioning cells and the construction of two-and three-dimensional synthetic tissues *Exp. Cell Res.* **179** 362–73
[20] Binder K W, Zhao W, Aboushwareb T, Dice D, Atala A and Yoo J J 2010 *In situ* bioprinting of the skin for burns *J. Am. Coll. Surg.* **211** S76
[21] Zhao Y, Yao R, Ouyang L, Ding H, Zhang T, Zhang K, Cheng S and Sun W 2014 Three-dimensional printing of hela cells for cervical tumor model *in vitro Biofabrication* **6** 035001
[22] Li C *et al* 2015 Rapid formation of a supramolecular polypeptide-DNA hydrogel for *in situ* three-dimensional multilayer bioprinting *Angew. Chem., Int. Ed. Engl.* **54** 3957–61
[23] Gruene M, Unger C, Koch L, Deiwick A and Chichkov B 2011 Dispensing pico to nanolitre of a natural hydrogel by laser-assisted bioprinting *Biomed. Eng. Online* **10** 19–30
[24] Cui X, Dean D, Ruggeri Z M and Boland T 2010 Cell damage evaluation of thermal inkjet printed Chinese hamster ovary cells *Biotechnol. Bioeng.* **106** 963–9

[25] Wang W, Huang Y, Grujicic M and Chrisey D B 2008 Study of impact-induced mechanical effects in cell direct writing using smooth particle hydrodynamic method *J. Manuf. Sci. Eng.* **130** 0210121–02101210
[26] Young D, Auyeung R C Y, Piqué A, Chrisey D B and Dlott D D 2001 Time-resolved optical microscopy of a laser-based forward transfer process *Appl. Phys. Lett.* **78** 3169–71
[27] Huang J, Cai R and Zhang K 2012 Experiments and analysis of drop on demand cell printing *Res. J. Appl. Sci.* **4**(**2**) 93–6
[28] Guillotin B and Guillemot F 2011 Cell patterning technologies for organotypic tissue fabrication *Trends Biotechnol.* **29** 183–90
[29] Barron J A, Wu P, Ladouceur H D and Ringeisen B R 2004 Biological laser printing: a novel technique for creating heterogeneous 3-dimensional cell patterns *Biomed. Microdevices* **6** 139–47
[30] Xu T, Jin J, Gregory C, Hickman J J and Boland T 2005 Inkjet printing of viable mammalian cells *Biomaterials* **26** 93–9
[31] Pardo L, Wilson W C and Boland T 2003 Characterization of patterned self-assembled monolayers and protein arrays generated by the ink-jet method *Langmuir* **19** 1462–6
[32] Calvert P 2001 Inkjet printing for materials and devices *Chem. Mater.* **13** 3299–305
[33] Wilson W C and Boland T 2003 Cell and organ printing 1: protein and cell printers *Anat. Rec.* **272A** 491–6
[34] Roth E A, Xu T, Das M, Gregory C, Hickman J J and Boland T 2004 Inkjet printing for high-throughput cell patterning *Biomaterials* **25** 3707–15
[35] Campbell P G and Weiss L E 2007 Tissue engineering with the aid of inkjet printers *Expert Opin. Biol. Ther.* **7** 1123–7
[36] Boland T, Mironov V, Gutowska A, Roth E A and Markwald R R 2003 Cell and organ printing 2: Fusion of cell aggregates in three-dimensional gels *Anat. Rec.* **272A** 497–502
[37] Faulkner-Jones A, Greenhough S, King J A, Gardner J, Courtney A and Shu W 2013 Development of a valve-based cell printer for the formation of human embryonic stem cell spheroid aggregates *Biofabrication* **5** 015013
[38] Faulkner A and Shu W 2012 Biological cell printing technologies *Nanotechnology Percept.* **8** 35–57
[39] Ozbolat I and Yu Y 2013 Bioprinting towards organ fabrication: challenges and future trends *IEEE Trans. Biomed. Eng.* **60** 691–9
[40] Snyder J E, Hamid Q, Wang C, Chang R, Emami K, Wu H and Sun W 2011 Bioprinting cell-laden matrigel for radioprotection study of liver by pro-drug conversion in a dual-tissue microfluidic chip *Biofabrication* **3** 034112
[41] Li M G, Tian X Y and Chen X B 2009 A brief review of dispensing-based rapid prototyping techniques in tissue scaffold fabrication: role of modeling on scaffold properties prediction *Biofabrication* **1** 032001
[42] Parsa S, Gupta M, Loizeau F and Cheung K C 2010 Effects of surfactant and gentle agitation on inkjet dispensing of living cells *Biofabrication* **2** 025003
[43] Ringeisen B R 2009 43: the evolution of cell printing *Fundamentals of Tissue Engineering and Regenerative Medicine* (Berlin: Springer) pp 613–31
[44] Nakamura M, Kobayashi A, Takagi F, Watanabe A, Hiruma Y, Ohuchi K, Iwasaki Y, Horie M, Morita I and Takatani S 2005 Biocompatible inkjet printing technique for designed seeding of individual living cells *Tissue Eng.* **11** 1658–66
[45] Vozzi G, Previti A, De Rossi D and Ahluwalia A 2002 Microsyringe-based deposition of two-dimensional and three-dimensional polymer scaffolds with a well-defined geometry for application to tissue engineering *Tissue Eng.* **8** 1089–98
[46] Melchels F P W, Domingos M A N, Klein T J, Malda J, Bartolo P J and Hutmacher D W 2012 Additive manufacturing of tissues and organs *Prog. Polym. Sci.* **37** 1079–104
[47] Liu Y, Cheng D K, Sonek G J, Berns M W, Chapman C F and Tromberg B J 1995 Evidence for localized cell heating induced by infrared optical tweezers *Biophys. J.* **68** 2137–44
[48] Barron J A, Krizman D B and Ringeisen B R 2005 Laser printing of single cells: statistical analysis, cell viability, and stress *Ann. Biomed. Eng.* **33** 121–30
[49] Ringeisen B R, Othon C M, Barron J A, Young D and Spargo B J 2006 Jet-based methods to print living cells *Biotechnol. J.* **1** 930–48
[50] Schiele N R, Corr D T, Huang Y, Raof N A, Xie Y and Chrisey D B 2010 Laser-based direct-write techniques for cell printing *Biofabrication* **2** 032001
[51] Koch L, Kuhn S, Sorg H, Gruene M, Schlie S, Gaebel R, Polchow B, Reimers K, Stoelting S and Ma N 2009 Laser printing of skin cells and human stem cells *Tissue Eng. C: Methods* **16** 847–54
[52] Barron J A, Ringeisen B R, Kim H, Spargo B J and Chrisey D B 2004 Application of laser printing to mammalian cells *Thin Solid Films* **453-454** 383–7
[53] Guillotin B *et al* 2010 Laser assisted bioprinting of engineered tissue with high cell density and microscale organization *Biomaterials* **31** 7250–6
[54] Duocastella M, Colina M, Fernández-Pradas J M, Serra P and Morenza J L 2007 Study of the laser-induced forward transfer of liquids for laser bioprinting *Appl. Surf. Sci.* **253** 7855–9
[55] Hopp B, Smausz T, Kresz N, Barna N, Bor Z, Kolozsvári L, Chrisey D B, Szabó A and Nógrádi A 2005 Survival and proliferative ability of various living cell types after laser-induced forward transfer *Tissue Eng.* **11** 1817–23
[56] Ellson R, Mutz M, Browning B, Lee L Jr, Miller M F and Papen R 2003 Transfer of low nanoliter volumes between microplates using focused acoustics—automation considerations *J. Assoc. Lab. Autom.* **8** 29–34
[57] Elrod S A, Hadimioglu B, Khuri-Yakub B T, Rawson E G, Richley E, Quate C F, Mansour N N and Lundgren T S 1989 Nozzleless droplet formation with focused acoustic beams *J. Appl. Phys.* **65** 3441–7
[58] Yan Y, Wang X, Pan Y, Liu H, Cheng J, Xiong Z, Lin F, Wu R, Zhang R and Lu Q 2005 Fabrication of viable tissue-engineered constructs with 3D cell-assembly technique *Biomaterials* **26** 5864–71
[59] Fedorovich N E, Alblas J, de Wijn J R, Hennink W E, Verbout A J and Dhert W J A 2007 Hydrogels as extracellular matrices for skeletal tissue engineering: state-of-the-art and novel application in organ printing *Tissue Eng.* **13** 1905–25
[60] Slaughter B V, Khurshid S S, Fisher O Z, Khademhosseini A and Peppas N A 2009 Hydrogels in regenerative medicine *Adv. Mater.* **21** 3307–29
[61] Kong H-J, Lee K Y and Mooney D J 2002 Decoupling the dependence of rheological/mechanical properties of hydrogels from solids concentration *Polymer* **43** 6239–46
[62] Peppas N A, Hilt J Z, Khademhosseini A and Langer R 2006 Hydrogels in biology and medicine: from molecular principles to bionanotechnology *Adv. Mater.* **18** 1345–60
[63] Shoichet M S, Li R H, White M L and Winn S R 1996 Stability of hydrogels used in cell encapsulation: an *in vitro* comparison of alginate and agarose *Biotechnol. Bioeng.* **50** 374–81
[64] Yu J, Du K T, Fang Q, Gu Y, Mihardja S S, Sievers R E, Wu J C and Lee R J 2010 The use of human mesenchymal stem cells encapsulated in RGD modified alginate microspheres in the repair of myocardial infarction in the rat *Biomaterials* **31** 7012–20
[65] Ortega Í, Deshpande P, Gill A A, MacNeil S and Claeyssens F 2013 Development of a microfabricated artificial limbus with micropockets for cell delivery to the cornea *Biofabrication* **5** 025008
[66] Levato R, Visser J, Planell J A, Engel E, Malda J and Mateos-Timoneda M A 2014 Biofabrication of tissue constructs by 3D bioprinting of cell-laden microcarriers *Biofabrication* **6** 035020
[67] Costa P F, Vaquette C, Baldwin J, Chhaya M, Gomes M E, Reis R L, Theodoropoulos C and Hutmacher D W 2014 Biofabrication of customized bone grafts by combination of additive manufacturing and bioreactor knowhow *Biofabrication* **6** 035006
[68] Nair K, Gandhi M, Khalil S, Yan K C, Marcolongo M, Barbee K and Sun W 2009 Characterization of cell viability during bioprinting processes *Biotechnol. J.* **4** 1168–77

[69] Aguado B A, Mulyasasmita W, Su J, Lampe K J and Heilshorn S C 2011 Improving viability of stem cells during syringe needle flow through the design of hydrogel cell carriers *Tissue Eng.* A **18** 806–15
[70] Kang K H, Hockaday L A and Butcher J T 2013 Quantitative optimization of solid freeform deposition of aqueous hydrogels *Biofabrication* **5** 035001
[71] Chang R, Nam J and Sun W 2008 Effects of dispensing pressure and nozzle diameter on cell survival from solid freeform fabrication–based direct cell writing *Tissue Eng.* A **14** 41–8
[72] Raof N A, Schiele N R, Xie Y and Chrisey D B 2011 The maintenance of pluripotency following laser direct-write of mouse embryonic stem cells *Biomaterials* **32** 1802–8
[73] Chen L and Daley G Q 2008 Molecular basis of pluripotency *Hum. Mol. Genetics* **17** R23–7
[74] Takebe T *et al* 2013 Vascularized and functional human liver from an iPSC-derived organ bud transplant *Nature* **499** 481–4
[75] Si-Tayeb K, Lemaigre F P and Duncan S A 2010 Organogenesis and development of the liver *Dev. Cell* **18** 175–89
[76] Marchioli G *et al* 2015 Fabrication of three-dimensional bioplotted hydrogel scaffolds for islets of Langerhans transplantation *Biofabrication* **7** 025009
[77] Dixon J E, Shah D A, Rogers C, Hall S, Weston N, Parmenter C D J, McNally D, Denning C and Shakesheff K M 2014 Combined hydrogels that switch human pluripotent stem cells from self-renewal to differentiation *Proc. Natl Acad. Sci.* **111** 5580–5